Available online at www.sciencedirect.com
SCIENCE DIRECT
Catalysis Today 116 (2006) 143–150
CATALYSIS TODAY
www.elsevier.com/locate/cattod

New solid superacid catalyst prepared by doping ZrO_2 with Ce and modifying with sulfate and its catalytic activity for acid catalysis

Jong Rack Sohn [a,*], Si Hoon Lee [b], Jun Seob Lim [a]

[a] Department of Applied Chemistry, Engineering College, Kyungpook National University, Taegu 702-701, Republic of Korea
[b] Environment Research Team, Research Institute of Industrial Science and Technology, Pohang 790-330, Republic of Korea

Received 7 October 2005; accepted 6 January 2006
Available online 30 May 2006

Abstract

A new solid superacid catalyst, Ce-ZrO_2/SO_4^{2-} was prepared simply by doping ZrO_2 with Ce and modifying with sulfate simultaneously. The characterization of prepared catalysts was performed using FTIR, XRD and DSC. The surface area of 5Ce-ZrO_2/SO_4^{2-} calcined at 650 °C was very high (121.2 m^2/g) compared to that of undoped and only sulfated ZrO_2 (56.0 m^2/g). This high surface area of Ce-ZrO_2/SO_4^{2-} was due to the doping effect of Ce, which makes zirconia a stable tetragonal phase as confirmed by XRD. 5Ce-ZrO_2/SO_4^{2-} containing 5 wt.% $Ce(SO_4)_2$ and calcined at 650 °C exhibited maximum catalytic activities for both reactions, 2-propanol dehydration and cumene dealkylation. The catalytic activities for both reactions were correlated with the acidity of catalysts measured by the ammonia chemisorption method. The role of Ce was to form a thermally stable solid solution with zirconia and consequently to give high surface area and acidity of the sample.

Keywords: Ce-ZrO_2/SO_4^{2-}; Acidity; Ce-doping; Modifying with sulfate; Cumene dealkylation; 2-Propanol dehydration

1. Introduction

Many kinds of solid acids have been found: their acidic properties, their catalysis and the structure of acid site have been elucidated and those results have been reviewed by several workers [1–4]. Solid acid catalysts are finding numerous applications in many areas. Liquid superacids based on HF, which are efficient and selective at room temperature, are not suitable for industrial processes due to separation problems tied with environmental regulations [5]. Many catalysts were reported in the literature including $AlCl_3$ with additives like $SbCl_3$ and HCl, chlorinated alumina, transition metal-exchanged zeolites, heteropoly acids and some bifunctional catalysts [6]. Most of these catalysts suffer from different drawbacks, such as high working temperature, continuous supply of chlorine and a high hydrogen pressure. Conventional industrial acid catalysts, such as sulfuric acid, $AlCl_3$ and BF_3, have unavoidable drawbacks because of their severe corrosivity and high susceptibility to water. Thus, the search for environmentally benign heterogeneous catalysts has driven the worldwide research of new materials as a substitute for current liquid acids and halogen-based solid acids. Among them sulfated oxides, such as sulfated zirconia, titania and iron oxide exhibiting high thermostability, superacidic property and high catalytic activity, have evoked increasing interest [2,3,7]. The strong acidity of zircona-supported sulfate has attracted much attention because of its ability to catalyze many reactions, such as cracking, alkylation, and isomerization.

In recent years, promoted zirconia catalysts have gained much attention for isomerization reactions due to their superacidity, non-toxicity and a high activity at low temperatures [3,8]. Sulfated zirconia incorporating Fe and Mn has been shown to be highly active for butane isomerization, catalyzing the reaction even at room temperature [9,10]. Such promotion in activity of catalyst has been confirmed by several other research groups [10–12]. Coelho et al. [13] have discovered that the addition of Ni to sulfated zirconia results in an activity enhancement comparable to that caused by the addition of Fe and Mn. It has been reported by several workers that the addition of platinum to zirconia modified by sulfate ions enhances catalytic activity in the skeletal isomerization of alkanes without deactivation when the reaction is carried out in the presence of hydrogen [14,15]. The high catalytic activity and small deactivation can be explained by both the elimination

* Corresponding author. Tel.: +82 53 950 5585; fax: +82 53 950 6594.
E-mail address: jrsohn@knu.ac.kr (J.R. Sohn).

0920-5861/$ – see front matter © 2006 Elsevier B.V. All rights reserved.
doi:10.1016/j.cattod.2006.01.023

of the coke by hydrogenation and hydrogenolysis, and the formation of Brönsted acid sites from H_2 on the catalysts [10]. Recently, it has been found that a main group element Al can also promote the catalytic activity and stability of sulfated zirconia for *n*-butane isomerization and ethylene dimerization [16–18].

The search for a more active catalyst is a never ending task. At the same time that increased catalytic activity is sought, an improvement in selectivity to the desired product is also required. It is known that for zirconia-supported catalyst its surface area and catalytic activity are decreasing under the severe reaction condition, such as high temperature above 600 °C. In this paper, we report new solid superacid catalyst prepared by doping ZrO_2 with Ce and modifying with sulfate simultaneously to improve catalytic activity and thermal stability. For the acid catalysis, the 2-propanol dehydration and cumene dealkylation were used as test reactions.

2. Experimental

2.1. Catalyst preparation

The precipitate of $Zr(OH)_4$ was obtained by adding aqueous ammonia slowly into an aqueous solution of zirconium oxychloride (Junsei Chemical Co.) at room temperature with stirring until the pH of mother liquor reached about 8. The preparation of catalyst doped with Ce and modified with sulfate simultaneously was carried out by adding an acidic aqueous solution of cerium sulfate $[Ce(SO_4)_2{\cdot}4H_2O]$ to the $Zr(OH)_4$ powder followed by drying and calcining at high temperatures for 2 h in air [19]. This series of catalysts is denoted by the weight percentage of $Ce(SO_4)_2$. For example, 5Ce-ZrO_2/SO_4^{2-} indicates the catalyst containing 5 wt.% of $Ce(SO_4)_2$.

2.2. Procedure

FTIR spectra were obtained in a heatable gas cell at room temperature using a Mattson Model GL6030E spectrophotometer. The self-supporting catalyst wafers contained about 9 mg cm^{-2}. Prior to obtaining the spectra, we heated each sample under vacuum at 25–500 °C for 1 h. Catalysts were checked in order to determine the structure of the prepared catalysts by means of a Philips X'pert-APD X-ray diffractometer, employing Ni-filtered Cu Kα radiation. DSC measurements were performed by a PL-STA model 1500H apparatus in air; the heating rate was 5 °C/min. For each experiment, 10–15 mg of sample was used.

The specific surface area was determined by applying the BET method to the adsorption of N_2 at −196 °C. Chemisorption of ammonia was also employed as a measure of the acidity of catalysts. The amount of chemisorption was determined based on the irreversible adsorption of ammonia [20–22].

2-Propanol dehydration was carried out at 160 °C in a pulse micro-reactor connected to a gas chromatograph. Fresh catalyst in the reactor made of 1/4 in. stainless steel was pretreated at 400 °C for 1 h in a nitrogen atmosphere. Diethyleneglycol succinate on shimalite was used as packing material of the gas chromatograph and the column temperature for analyzing the product was 150 °C. Catalytic activity for 2-propanol dehydration was represented as mole of propylene converted from 2-propanol per gram of catalyst. Cumene dealkylation was carried out at 400 °C in the same reactor as above. Packing material for the gas chromatograph was Bentone 34 on chromosorb W and column temperature was 130 °C. Catalytic activity for cumene dealkylation was represented as mole of benzene converted from cumene per gram of catalyst. The average of the first to sixth pulse values were taken as the conversions for both reactions.

3. Results and discussion

3.1. Infrared spectra

The infrared spectra of 3Ce-ZrO_2/SO_4^{2-} (KBr disc) calcined at different temperatures (300–800 °C) are given in Fig. 1. 3Ce-ZrO_2/SO_4^{2-} calcined up to 700 °C showed infrared absorption bands at 1283, 1222, 1142 and 1096 cm^{-1}, which are assigned to bidentate sulfate ions coordinated to the metal, such as ZrO_2 [22,23]. The band at 1625 cm^{-1} is assigned to the deformation

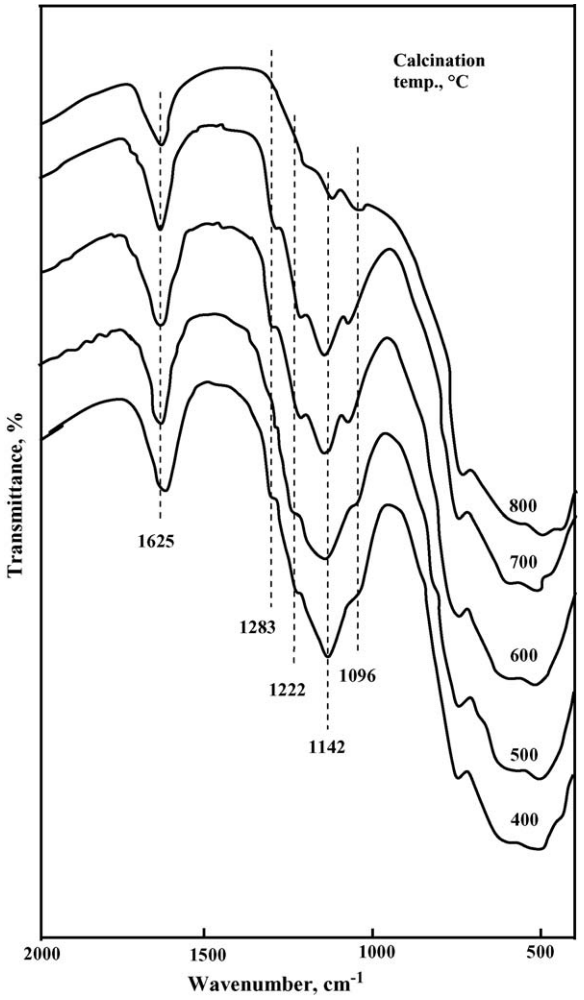

Fig. 1. Infrared spectra of 5Ce-ZrO_2/SO_4^{2-} calcined at different temperatures for 2 h.

vibration mode of the adsorbed water. For 3Ce-ZrO_2/SO_4^{2-} calcined at 700 °C, the band intensities of sulfate ion decreased because of the partial decomposition of sulfate ion. However, for the sample calcined at 800 °C, infrared bands ascribed to the sulfate ion disappeared due to the decomposition of sulfate ion.

In general, for the metal oxides modified with sulfate ions followed by evacuation above 400 °C, a strong band assigned to S=O stretching frequency is observed at 1360–1410 cm^{-1} [23–25]. The infrared spectra of self-supported 3Ce-ZrO_2/SO_4^{2-} after evacuation at different temperatures for 1 h were examined. As shown in Fig. 2, there are sharp bands at 1364–1390 cm^{-1} accompanied by four broad but split bands at 900–1200 cm^{-1}, indicating the presence of two kinds of sulfated species. The bands at 1364–1390 cm^{-1} correspond to the asymmetric S=O stretching frequency of sulfate ion bonded to ZrO_2 under the dehydrated condition, while the latter four bands are assigned to bidentate sulfate ion coordinated to ZrO_2 [25,26]. Such results are very similar to those of other workers [24,26]. However, the frequency shift of this band is different depending on the evacuation temperature, as shown in Fig. 2. At 100 °C an asymmetric stretching band of S=O bonds was not observed, because the water molecules are adsorbed on the surface of 3Ce-ZrO_2/SO_4^{2-} [25,26]. However, from 200 °C the band began to appear at 1364 cm^{-1}; the band intensity increased with the evacuation temperature and the position of band shifted to a higher wavenumber. That is, the higher the evacuation temperature, the larger the shift of the asymmetric stretching frequency of the S=O bonds. It is likely that the surface sulfur complexes formed by the interaction of oxides with sulfate ions in highly active catalysts have a strong tendency to reduce their bond order by the adsorption of basic molecules, such as H_2O [25,26]. Consequently, as shown in Fig. 2, an asymmetric stretching band of S=O bonds for the sample evacuated at lower temperature appears at a lower frequency compared with that for the sample evacuated at higher temperature, because the adsorbed water reduces the bond order of S=O from a highly covalent double-bond character to a lesser double-bond character. Therefore, it is obvious that the asymmetric stretching frequencies of the S=O bonds are related to the acidic properties as discussed later.

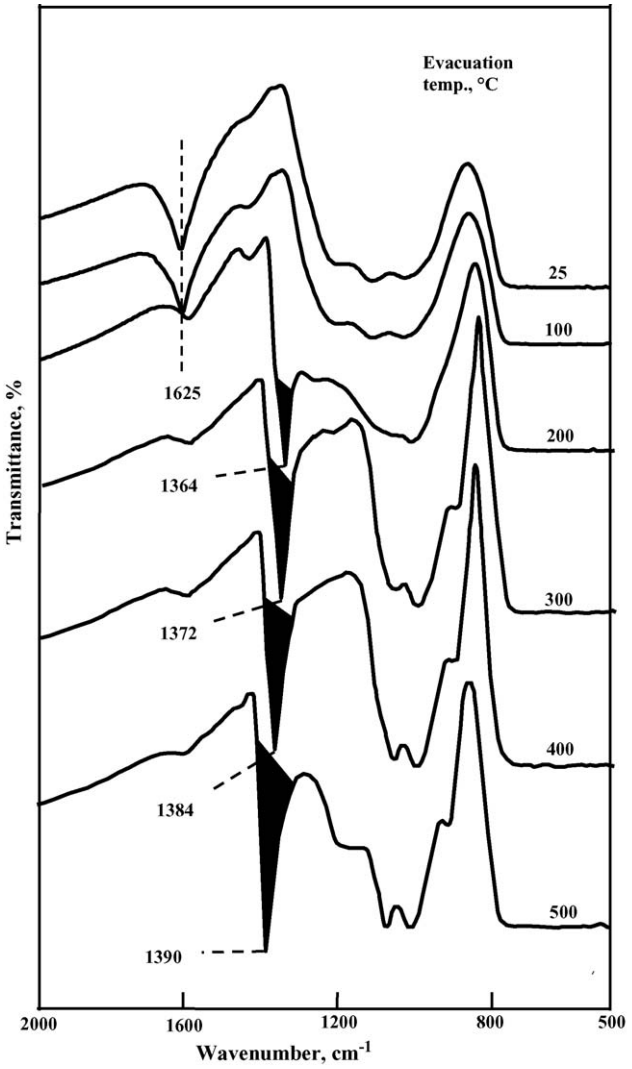

Fig. 2. Infrared spectra of 5Ce-ZrO_2/SO_4^{2-} evacuated at different temperatures for 1 h.

3.2. Crystalline structures of catalysts

The crystalline structures of catalysts calcined in air at different temperatures for 2 h were examined. With zirconia support, as shown in Fig. 3, ZrO_2 was amorphous to XRD up to 300 °C, tetragonal phase at 350 °C, a two-phase mixture of the tetragonal and monoclinic forms at 400–800 °C, and a

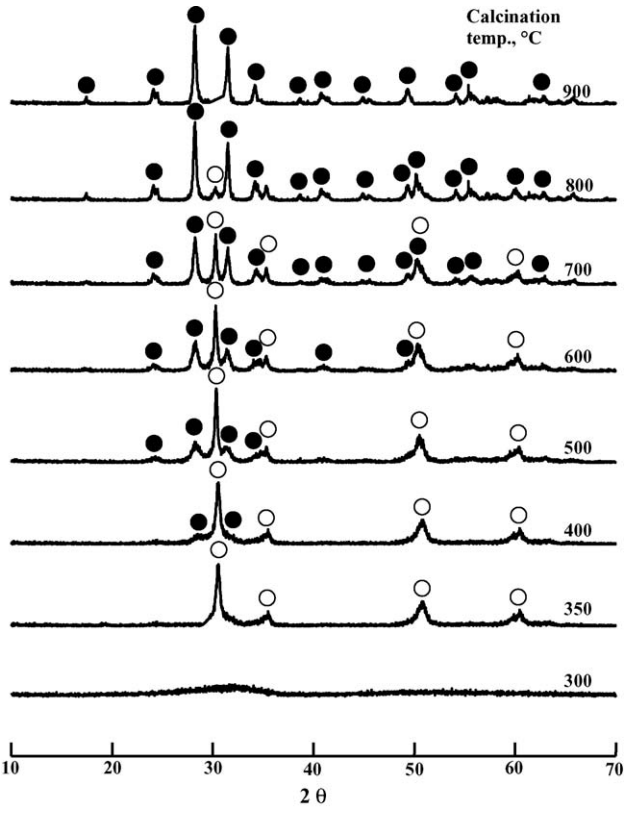

Fig. 3. X-ray diffraction patterns of ZrO_2 calcined at different temperatures for 2 h: (○) tetragonal phase of ZrO_2; (●) monoclinic phase of ZrO_2.

monoclinic phase at 900 °C. Three crystal structures of ZrO_2, i.e., tetragonal, monoclinic and cubic phases have been reported [18,21,26].

However, in Ce-ZrO_2/SO_4^{2-} catalysts, the crystalline structures of the samples are different from that of the ZrO_2 support. The 5Ce-ZrO_2/SO_4^{2-} and 10Ce-ZrO_2/SO_4^{2-} catalysts calcined at different temperatures for 2 h, as shown in Figs. 4 and 5, are amorphous up to 500 °C. In other words, the transition temperature of ZrO_2 from amorphous to tetragonal phase was higher by 250 °C for Ce-ZrO_2/SO_4^{2-} catalysts than for pure ZrO_2 [20]. X-ray diffraction data for two samples indicated only the tetragonal phase of ZrO_2 at 600–650 °C and a two-phase mixture of the tetragonal and monoclinic forms at 700–800 °C. It is assumed that the interaction between $Ce(SO_4)_2$ and ZrO_2 hinders the phase transition of ZrO_2 from amorphous to tetragonal [16,18,23]. For the above Ce-ZrO_2/SO_4^{2-} catalysts, there are no characteristic peaks of $Ce(SO_4)_2$ in the patterns, implying that $Ce(SO_4)_2$ is sufficiently homogeneously mixed with zirconia. The other Ce-ZrO_2/SO_4^{2-} catalysts also exhibited similar X-ray diffraction patterns to that of 5Ce-ZrO_2/SO_4^{2-}.

3.3. Thermal analysis

The X-ray diffraction patterns in Figs. 4 and 5 clearly show that the structures of Ce-ZrO_2/SO_4^{2-} are different depending on the calcined temperature. To examine the thermal properties of precursors for Ce-ZrO_2/SO_4^{2-} samples more clearly, we completed their thermal analysis; the results are illustrated in Fig. 6. For pure ZrO_2, the DSC curve shows a broad

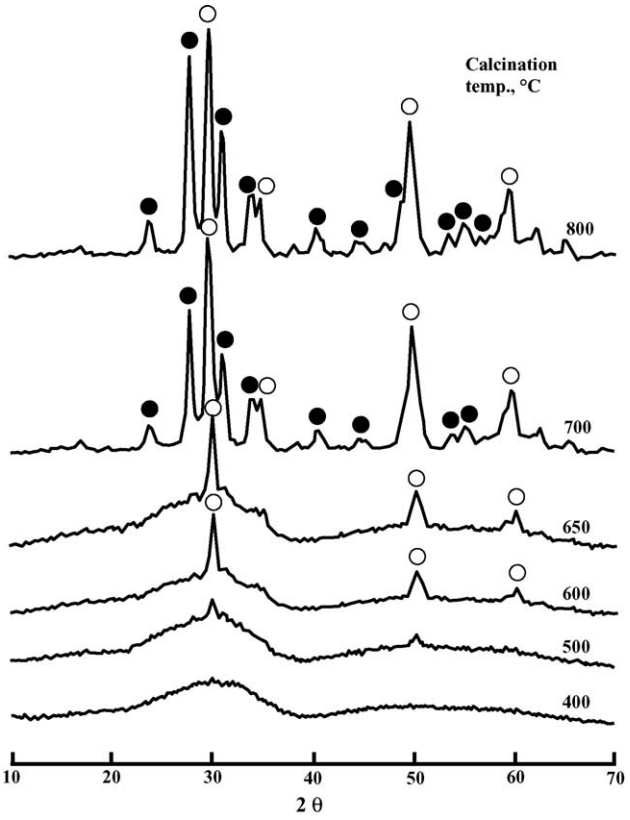

Fig. 5. X-ray diffraction patterns of 10Ce-ZrO_2/SO_4^{2-} calcined at different temperatures for 2 h: (○) tetragonal phase of ZrO_2; (●) monoclinic phase of ZrO_2.

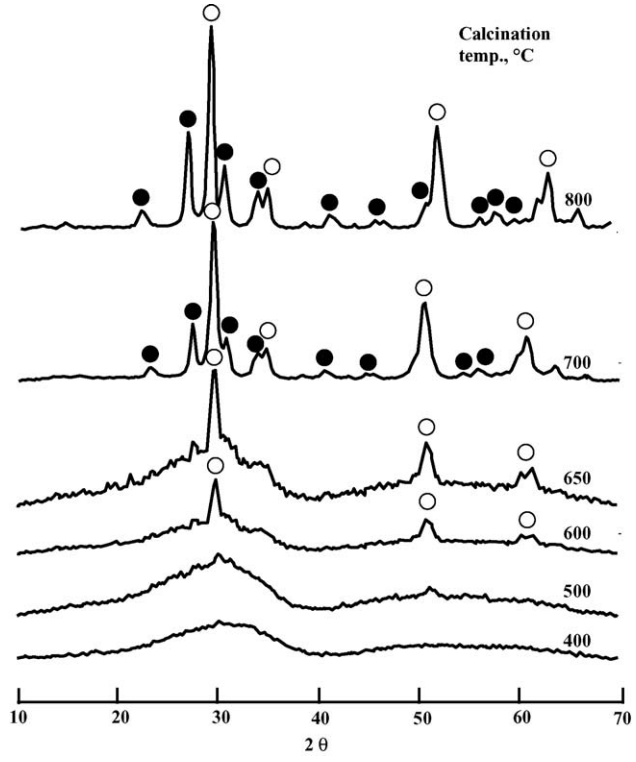

Fig. 4. X-ray diffraction patterns of 5Ce-ZrO_2/SO_4^{2-} calcined at different temperatures for 2 h: (○) tetragonal phase of ZrO_2; (●) monoclinic phase of ZrO_2.

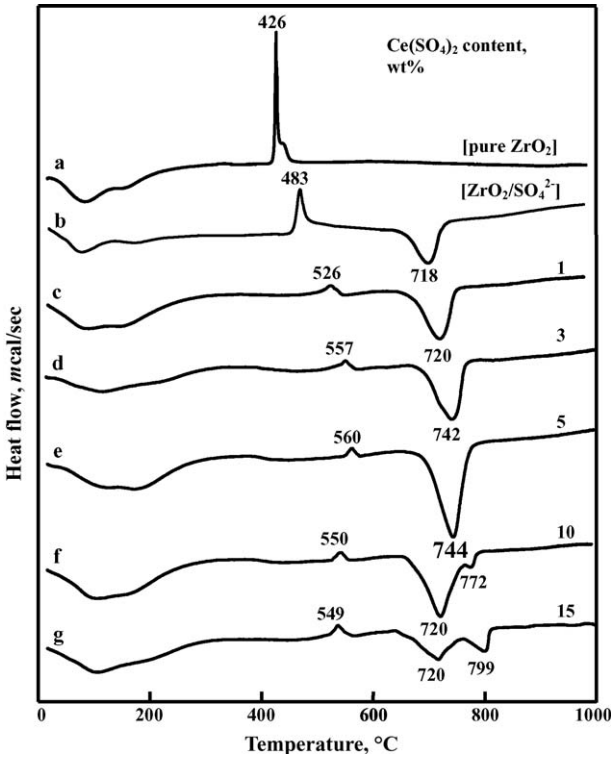

Fig. 6. DSC curves of Ce-ZrO_2/SO_4^{2-} precursors having different $Ce(SO_4)_2$ contents: (a) ZrO_2, (b) ZrO_2/SO_4^{2-}, (c) 1Ce-ZrO_2/SO_4^{2-}, (d) 3Ce-ZrO_2/SO_4^{2-}, (e) 5Ce-ZrO_2/SO_4^{2-}, (f) 10Ce-ZrO_2/SO_4^{2-} and (g) 15Ce-ZrO_2/SO_4^{2-}.

endothermic peak below 200 °C due to water elimination, and a sharp exothermic peak at 426 °C due to the phase transition of ZrO_2 from amorphous to tetragonal [18,23]. However, it is of interest to see the influence of doped-Ce and sulfate species on the crystallization of ZrO_2 from amorphous to tetragonal phase. As Fig. 6 shows, for ZrO_2/SO_4^{2-} and Ce-ZrO_2/SO_4^{2-} samples it is shifted to higher temperatures due to the interaction between $Ce(SO_4)_2$ and ZrO_2. Consequently, the exothermic peak appear at 483 °C for ZrO_2/SO_4^{2-}, 520 °C for 1Ce-ZrO_2/SO_4^{2-}, 557 °C for 3Ce-ZrO_2/SO_4^{2-} and 560 °C for 5Ce-ZrO_2/SO_4^{2-}. The endothermic peaks at 720–799 °C for Ce-ZrO_2/SO_4^{2-} samples are due to the evolution of SO_3 decomposed from sulfate species bonded to the surface of Ce-doped ZrO_2 [16,27]. The decomposition temperature depends on the amount of doped-Ce and sulfate species. The temperature increases with increasing Ce content up to 5 wt.%, indicating an increase in the thermal stability of the surface sulfate species with Ce content up to 5%. For 10Ce-ZrO_2/SO_4^{2-} and 15 Ce-ZrO_2/SO_4^{2-} samples containing high $Ce(SO_4)_2$ content, two peaks are observed, showing that sulfate species with different thermal stability are present in the samples.

3.4. Surface properties

Fig. 7 shows the BET surface areas of 5Ce-ZrO_2/SO_4^{2-} and 10Ce-ZrO_2/SO_4^{2-} as a function of calcination temperature. It was found surprisingly that the surface areas of catalysts calcined at 650–700 °C are very high compared to those calcined at 400–600 °C. This high surface area of Ce-ZrO_2/SO_4^{2-} is due to the doping effect of Ce, which makes zirconia a stable tetragonal phase [28] as confirmed by XRD. It was also reported that a small amount of rare-earth elements in zirconia powder can stabilize the tetragonal and cubic phases over a wide range of temperatures [29]. The surface area of 5Ce-ZrO_2/SO_4^{2-} calcined at 650 °C is 121.2 m^2/g (Table 1), whereas those of undoped pure ZrO_2 and only sulfated ZrO_2 are 38 and 56 m^2/g, respectively. However, as shown in Fig. 4, the phase of catalyst calcined at 400–600 °C was mainly amorphous or poor crystalline of tetragonal phase. The role of Ce in the catalysts is to form a thermally stable solid solution with zirconia and consequently to give their high surface area [28,29].

Table 1
Specific surface area and acidity of 5Ce-ZrO_2/SO_4^{2-} catalysts calcined at different temperatures

Calcination temperature (°C)	Surface area (m^2/g)	Acidity (μmol/g)
400	29.4	46.2
500	31.0	51.3
600	41.2	57.4
650	121.2	129.3
700	102.1	107.2
800	48.3	62.3

Infrared spectroscopic studies of ammonia adsorbed on solid surfaces have made it possible to distinguish between Brönsted and Lewis acid sites [27,30–32]. Fig. 8 shows the infrared spectra of ammonia adsorbed on 3Ce-ZrO_2/SO_4^{2-} sample evacuated at 500 °C for 1 h. For 3Ce-ZrO_2/SO_4^{2-}, the band at 1444 cm^{-1} is the characteristic peak of ammonium ion, which is formed on the Brönsted acid sites. The absorption peak at 1620 cm^{-1} is contributed by ammonia coordinately bonded to

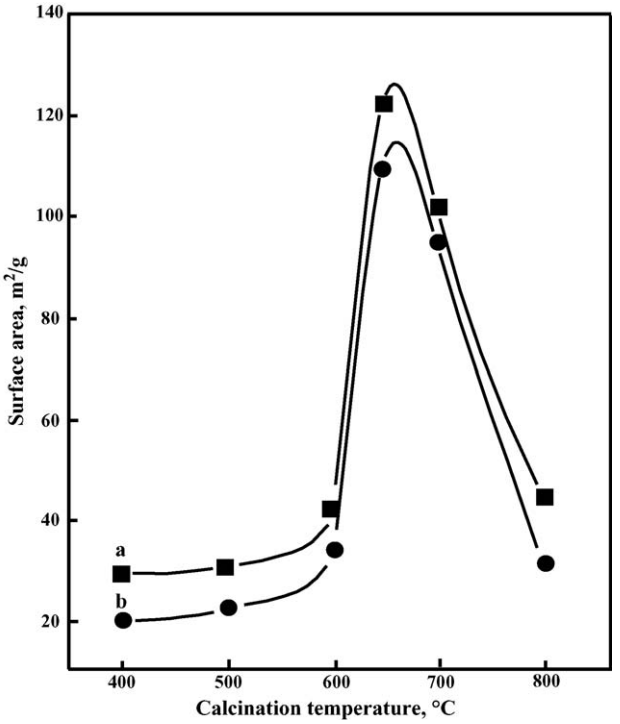

Fig. 7. Variations for surface area of 5Ce-ZrO_2/SO_4^{2-} (a) and 10Ce-ZrO_2/SO_4^{2-} (b) as a function of calcination temperature.

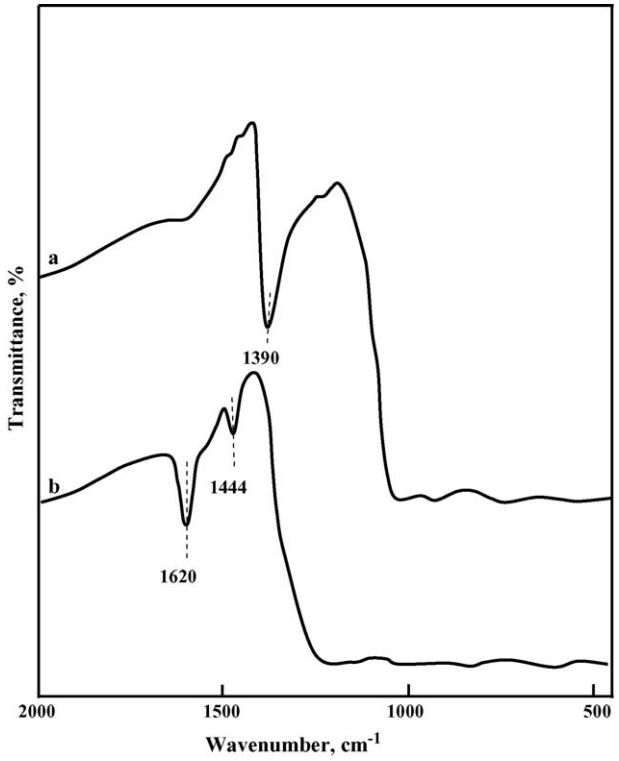

Fig. 8. Infrared spectra of NH_3 adsorbed on 3Ce-ZrO_2/SO_4^{2-}: (a) background of 3Ce-ZrO_2/SO_4^{2-} after evacuation at 500 °C for 1 h and (b) NH_3 adsorbed on (a), where gas was evacuated at 230 °C for 1 h.

Lewis acid sites [27,30–32], indicating the presence of both Brönsted and Lewis acid sites on the surface of 3Ce-ZrO_2/SO_4^{2-} sample. Other samples having different cerium sulfate contents also showed the presence of both Lewis and Brönsted acids. As Fig. 8(a) shows, the intense band at 1390 cm^{-1} after evacuation at 500 °C is assigned to the asymmetric stretching vibration of S=O bonds having a high double-bond nature [25,27]. However, a drastic shift of the infrared band from 1390 cm^{-1} to a lower wavenumber (not shown due to the overlaps of skeletal vibration bands of ZrO_2) after ammonia adsorption (Fig. 8(b)) indicates a strong interaction between an adsorbed ammonia molecule and the surface complex. Namely, the surface sulfur compound in the highly acidic catalysts has a strong tendency to reduce the bond order of S=O from a highly covalent double-bond character to a lesser double-bond character when a basic ammonia molecule is adsorbed on the catalysts [25,27].

The acid strength of the catalysts was examined by a color change method, using Hammett indicator [21,33] in sulfuryl chloride. The 5Ce-ZrO_2/SO_4^{2-} sample after evacuation at 500 °C for 1 h was estimated to have $H_0 \leq -14.5$, indicating the formation of superacidic sites. Acids stronger than $H_0 \leq -11.93$, which corresponds to the acid strength of 100% H_2SO_4, are superacids [2,3,25,35]. Consequently, Ce-ZrO_2/SO_4^{2-} catalysts would be solid superacids in analogy with the case of metal oxides modified with a sulfate group [7,25,34]. The superacidic property is attributed to the double-bond nature of the S=O in the complex formed by the interaction of Ce-ZrO_2 with sulfate. In other words, the acid strength of Ce-ZrO_2/SO_4^{2-} becomes stronger by the inductive effect of S=O in the complex [2,7,25,34].

3.5. Model structure for the acid sites

Numerous model structures have been reported for the acid sties in sulfated metal oxide. In particular, the surface acidity characterization of sulfated zirconia shows that its surface contains very strong Brönsted as well as Lewis acid sites. The number and the strength of these sites largely vary with parameters, such as sulfur concentration, activation temperature and surface area of the precursor oxide. Using IR spectroscopy, Tanabe and co-workers proposed a structure for acid site on sulfated metal oxides to be chelating bidentate complexes [34,36,37]. The central metal ion acts as a Lewis acid site, whose acid strength can be strongly influenced by the inductive effect of S=O in the sulfur complex. Arata proposed a structure for acid site on sulfated zirconia to be bridging bidentated state [3,38]. They observed that Lewis and Brönsted sites on sulfated zirconia are easily changeable by adsorption or desorption of water molecules. Saur et al. postulated that in the absence of water three oxygens of the sulfate are bonded to Al or Ti [39], whereas in the presence of water this is converted to a bridged bidentate sulfate, thus accounting for the increased amount of Brönsted acid site.

We can summarize the experimental results to suggest the model structure for the acid sites as following. Ce in the catalyst forms a thermally stable solid solution with zirconia. The decomposition temperature of sulfate species bonded to the surface of Ce-doped ZrO_2 increased with increasing Ce content up to 5 wt.%, indicating an increase in the thermal stability of the sulfate species in these samples. Infrared spectra of ammonia adsorbed on Ce-ZrO_2/SO_4^{2-} indicate the presence of both Bönsted and Lewis acid sites on the surface of Ce-ZrO_2/SO_4^{2-} sample. For the Ce-ZrO_2/SO_4^{2-} sample evacuated at 500 °C, the strong infrared band assigned to asymmetric S=O stretching frequency was observed at 1390 cm^{-1}, which demonstrates the superacidic property of Ce-ZrO_2/SO_4^{2-} sample [2,34]. Using Hammett indicator, the acid strength of Ce-ZrO_2/SO_4^{2-} sample after evacuation at 500 °C for 1 h was found to be $H_0 \leq -14.5$, indicating formation of superacidic sites on the surface of Ce-ZrO_2/SO_4^{2-}. From the above results and evidences, we suggest a model structure for the acid sites on Ce-ZrO_2/SO_4^{2-} as following scheme [19]. The Brönsted acid sites result from the weakening of the O–H bond by the inductive effect of neighboring sulfate groups, whereas the Lewis acid sites (Zr^+) are electronically deficient Zr^{4+} centers as a result of the electron-withdrawing nature of the sulfate group [34,37,40].

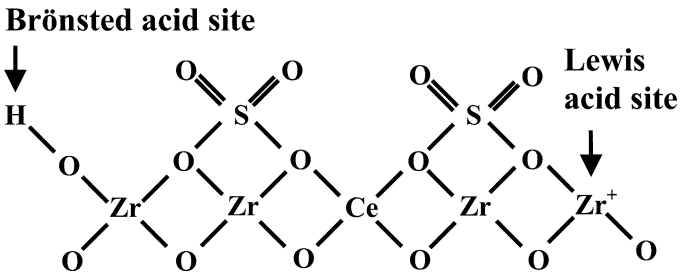

3.6. Catalytic activities for acid catalysis

Catalytic activities of 3Ce-ZrO_2/SO_4^{2-} for 2-propanol dehydration and cumene dealkylation are plotted as a function of calcination temperature in Fig. 9. The activities for both reactions increased with the calcination temperature, reaching a maximum at 650 °C, after which the activities decreased. The decrease of activities for both reactions above 650 °C can be attributed to the fact that the surface area and acidity above 650 °C decrease with the calcination temperature.

It is interesting to examine how catalytic activity of acid catalyst depends on the acid property. In view of Table 1 and Fig. 9, the variations in catalytic activities for both reactions can be correlated with the changes of their acid amount, showing the highest activity and acidity for 5Ce-ZrO_2/SO_4^{2-}. It has been known that 2-propanol dehydration takes place very readily on weak acid sites, while cumene dealkylation takes place on relatively strong acid sites of the catalysts [31,41]. Good correlations have been found in many cases between the acidity and the catalytic activities of solid acids [27,42,43].

It is confirmed that the catalytic activity gives a maximum at the calcination temperature of 650 °C. This seems to be closely correlated to the high surface area and high acidity of catalysts due to the formation of thermally stable solid solution between

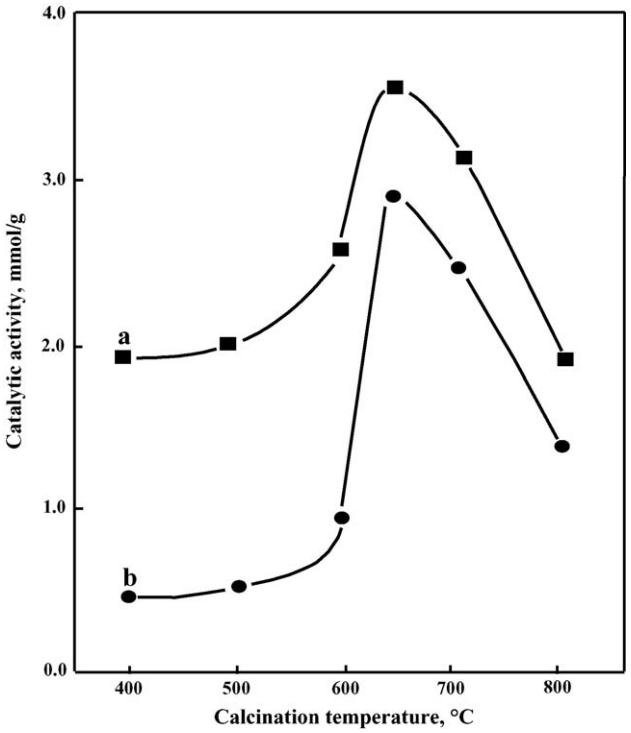

Fig. 9. Catalytic activity of 5Ce-ZrO_2/SO_4^{2-} for 2-propanol dehydration (a) and cumene dealkylation (b) as a function of calcination temperature.

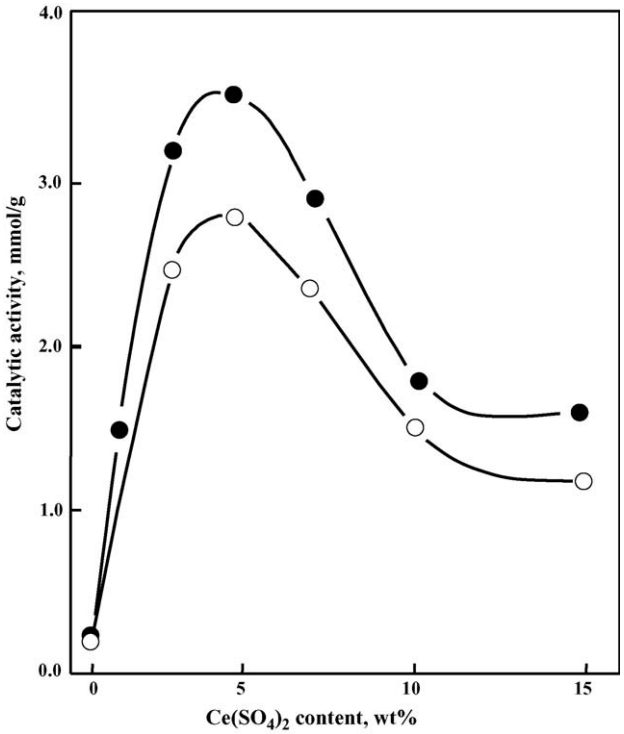

Fig. 10. Catalytic activities of Ce-ZrO_2/SO_4^{2-} for 2-propanol dehydration and cumene dealkylation as a function of $Ce(SO_4)_2$ content: (●) for 2-propanol dehydration; (○) for cumene dealkylation.

Ce and ZrO_2. As listed in Table 1, both BET surface area and acidity attained a maximum extent when the calcination temperature was 650 °C and then showed a gradual decrease with increasing the temperature. The correlation between catalytic activity and acidity holds for both reactions, 2-propanol dehydration and cumene dealkylation, although the acid strength required to catalyze acid reaction is different depending on the type of reactions.

We treated catalysts at 400 °C for 1 h in a nitrogen atmosphere before catalytic reactions. As shown in Fig. 2, the higher the evacuation temperature, the larger the shift of the asymmetric stretching frequency of the S=O bonds. An asymmetric frequency in the S=O bonds is a measure of the ability of a sulfur complex to pull basic molecules, such as NH_3 and H_2O and is a driving force in generating highly acidic properties, acid strength and acid amount [16,24,31]. Both acid strength and acid amount increase with an increase in the treatment temperature up to 500 °C, because water adsorbed on the catalyst surface is desorbed at high temperature, resulting in the formation of new acid sites and the increased bonds order of S=O. Therefore, the high catalytic activities of catalysts after heat-treatment at 400 °C is related to the shift of the asymmetric stretching frequency of the S=O bonds.

3.7. Effect of Ce-doping on catalytic activities

The catalytic activities of Ce-ZrO_2/SO_4^{2-} as a function of $Ce(SO_4)_2$ content for the reactions of 2-propanol dehydration and cumene dealkylation were examined, where the catalysts were pretreated at 400 °C for 1 h before reaction; the results are shown in Fig. 10. The catalytic activities for both reactions increased with increasing the $Ce(SO_4)_2$ content, reaching a maximum at 5 wt.%.

In general, it is known that a small amount of rare-earth solutes in nanophase zirconia powders can stabilize the tetragonal and cubic phases over a wide range of temperatures [44]. Considering the experimental results of Table 2 and Fig. 10, it seems likely that the catalytic activities for both reactions closely relates to the change of acidity of catalysts. As listed in Table 2, the total acid sites of 5Ce-ZrO_2/SO_4^{2-} and ZrO_2/SO_4^{2-} are 129.3 and 69.1 μmol/g, respectively, showing that the number of acid sites for the catalyst doped with Ce is greater than that for undoped catalyst. This high surface area and acidity are due to the Ce-doping effect, which makes zirconia tetragonal phase as confirmed by XRD, as shown in Figs. 4 and 5. This is consistent with the results reported by Roh et al. over Ce-doped Ni/Ce-ZrO_2 [45]. The

Table 2
Specific surface area and acidity of Ce-ZrO_2/SO_4^{2-} containing different $Ce(SO_4)_2$ and calcined at 650 °C

Catalyst	SO_3 content (wt.%)	Surface area (m^2/g)	Acidity (μmol/g)
ZrO_2/SO_4^{2-}	1.4	56.0	69.1
1Ce-ZrO_2/SO_4^{2-}	1.9	96.1	102.0
3Ce-ZrO_2/SO_4^{2-}	2.4	106.0	108.0
5Ce-ZrO_2/SO_4^{2-}	2.8	121.2	129.3
7Ce-ZrO_2/SO_4^{2-}	3.3	114.0	118.0
10Ce-ZrO_2/SO_4^{2-}	4.6	107.0	113.0
15Ce-ZrO_2/SO_4^{2-}	5.1	91.3	99.6

doping effect of Ce is related to an increase in number of surface acidic sites.

The formation of solid solution, Ce-ZrO_2 results in an increase in the thermal stability of the surface sulfate species and consequently the acidity of Ce-doped catalyst is increased. In fact, to examine the thermal stability of the surface sulfate species DSC measurements were carried out (Fig. 6). The endothermic peak due to the evolution of SO_3 decomposed from sulfate species bonded to the surface of ZrO_2 appeared at 718 °C, while that from sulfate species bonded to the surface of Ce-doped ZrO_2 appeared at 744 °C. Such a temperature difference has been attributed to the stabilizing effect of the Ce dopant on the sulfate species. The Ce-ZrO_2 solid solution leads to an increase in the thermal stability of the surface sulfate species and consequently the acidity of the catalysts is increased.

SO_3 content estimated from TGA curves is also listed in Table 2 in order to examine the effect of SO_3 content on the acidity as well as catalytic activity. Based on the results of Table 2 and Fig. 10, both acidity and catalytic activities increased with increasing SO_3 content up to 2.8 wt.%. However, for catalysts containing SO_3 content above 2.8 wt.% both their acidity and catalytic activities rather decreased, indicating that there is an optimum content of SO_3 (2.8 wt.%) for the best catalyst to be prepared.

4. Conclusions

A new solid superacid catalyst, Ce-ZrO_2/SO_4^{2-} was prepared by doping ZrO_2 with Ce and modifying with sulfate simultaneously. The surface areas of catalysts calcined at 650 °C were very high compared to those of catalysts calcined at 400–600 °C, which was due to the doping effect of Ce which made zirconia a thermally stable tetragonal phase as confirmed by XRD. The formation of solid solution between Ce and ZrO_2 resulted in an increase in the thermal stability of the sulfate species bonded to the surface of Ce-ZrO_2 and consequently the acid amount and catalytic activities of catalyst were increased. The high catalytic activities of catalysts after heat-treatment at 400 °C is related to the shift of the asymmetric stretching frequency of the S=O bonds of sulfate species. The correlation between catalytic activity and acidity holds for both reactions, 2-propanol dehydration and cumene dealkylation.

Acknowledgements

This work was supported by the Korea Research Foundation Grant (KRF-2004-041-D00170). We wish to thank Korea Basic Science Institute (Daegu Branch) for the use of X-ray diffractometer.

References

[1] J.R. Sohn, J. Ind. Eng. Chem. 10 (2004) 1.
[2] K. Tanabe, M. Misono, Y. Ono, H. Hattori, New Solid Acids and Bases, Elsevier Science, Amsterdam, 1989 (Chapter 4).
[3] K. Arata, Adv. Catal. 37 (1990) 165.
[4] B.H. Davis, R.A. Keogh, R. Srinivasan, Catal. Today 20 (1994) 219.
[5] G.A. Olah, G.K.S. Prakash, J. Sommer, Superacids, Wiley-Interscience, NY, U.S.A., 1985, pp. 33–52.
[6] Y. Ono, Catal. Today 81 (2003) 3.
[7] J.R. Sohn, S.H. Lee, Appl. Catal. A: Gen. 266 (2004) 89.
[8] K. Arata, Appl. Catal. A: Gen. 146 (1996) 3.
[9] C.Y. Hsu, C.R. Heimbuch, C.T. Armes, B.C. Gates, J. Chem. Soc., Chem. Commun. (1992) 1645.
[10] V. Adeeva, H.W. de Haan, J. Janchen, G.D. Lei, V. Schunemann, L.J.M. van de Ven, W.M.H. Sachtler, R.A. van Santen, J. Catal. 151 (1995) 364.
[11] K.T. Wan, C.B. Khouw, M.E. Davis, J. Catal. 158 (1996) 311.
[12] X. Song, K.R. Reddy, A. Sayari, J. Catal. 161 (1996) 206.
[13] M.A. Coelho, D.E. Resasco, E.C. Sikabwe, R.L. White, Catal. Lett. 32 (1995) 253.
[14] K. Ebitani, J. Konishi, H. Hattori, J. Catal. 130 (1991) 257.
[15] M. Signoretto, F. Pinna, G. Strukul, P. Chies, G. Cerrato, S.D. Ciero, C. Morterra, J. Catal. 167 (1997) 522.
[16] W. Hua, Y. Xia, Y. Yue, Z. Gao, J. Catal. 196 (2000) 104.
[17] J.A. Moreno, G. Poncelet, J. Catal. 203 (2001) 153.
[18] J.R. Sohn, E.S. Cho, Appl. Catal. A: Gen. 282 (2005) 147.
[19] J.R. Sohn, J.S. Lim, S.H. Lee, Chem. Lett. 33 (2004) 1490.
[20] J.R. Sohn, W.C. Park, Appl. Catal. A: Gen. 230 (2002) 11.
[21] J.R. Sohn, S.G. Cho, Y.I. Pae, S. Hayashi, J. Catal. 159 (1996) 170.
[22] J.R. Sohn, D.H. Seo, S.H. Lee, J. Ind. Eng. Chem. 10 (2004) 309.
[23] J.R. Sohn, J.G. Kim, T.D. Kwon, E.H. Park, Langmuir 18 (2002) 1666.
[24] O. Saur, M. Bensitel, A.B.M. Saad, J.C. Lavalley, C.P. Tripp, B.A. Morrow, J. Catal. 99 (1986) 104.
[25] T. Yamaguchi, Appl. Catal. 61 (1990) 1.
[26] G. Larsen, E. Lotero, L.M. Petkovic, D.S. Shobe, J. Catal. 169 (1997) 67.
[27] J.R. Sohn, W.C. Park, Appl. Catal. A: Gen. 239 (2003) 269.
[28] W.-S. Dong, H.-S. Roh, K.-W. Jun, S.-E. Park, Y.-S. Oh, Appl. Catal. A 226 (2002) 63.
[29] C.-K. Loong, M. Ozawa, J. Alloys Compd. 303–304 (2000) 60.
[30] A. Satsuma, A. Hattori, K. Mizutani, A. Furuta, A. Miyamoto, T. Hattori, Y. Murakami, J. Phys. Chem. 92 (1988) 6052.
[31] J.R. Sohn, S.H. Lee, Appl. Catal. A: Gen. 266 (2004) 89.
[32] J.R. Sohn, J.S. Han, J. Ind. Eng. Chem. 11 (2005) 439.
[33] J.R. Sohn, S.G. Ryu, Langmuir 9 (1993) 126.
[34] T. Jin, T. Yamaguchi, K. Tananbe, J. Phys. Chem. 90 (1986) 4794.
[35] F.G.A. Olah, G.K.S. Prakash, J. Sommer, Science 206 (1979) 13.
[36] T. Jin, M. Machida, T. Yamaguchi, K. Tanabe, Inorg. Chem. 23 (1984) 4396.
[37] T. Yamaguchi, T. Jin, K. Tanabe, J. Phys. Chem. 90 (1986) 3148.
[38] K. Arata, Mater. Chem. Phys. 26 (1990) 213.
[39] O. Saur, M. Bensitel, A.B. Mohammed Saad, J.C. Lavalley, C.P. Tripp, B.A. Morrow, J. Catal. 99 (1986) 104.
[40] B.M. Reddy, P.M. Sreekanth, Y. Yamada, Q. Xu, T. Kobayashi, Appl. Catal. A: Gen. 228 (2002) 269.
[41] S.J. Decanio, J.R. Sohn, P.O. Fritz, J.H. Lunsford, J. Catal. 101 (1986) 132.
[42] K. Tanabe, Solid Acids and Bases, Kodansha, Tokyo, 1970 (Chapter 5).
[43] J.R. Sohn, A. Ozaki, J. Catal. 61 (1980) 291.
[44] C.-K. Loong, J.W. Richardson Jr., M. Ozawa, J. Catal. 157 (1995) 636.
[45] H.-S. Roh, W.-S. Dong, K.-W. Jun, S.-E. Park, Chem. Lett. (2001) 88.